Identification of pollen-expressed pectin methylesterase inhibitors in *Arabidopsis*

Sebastian Wolf, Slobodanka Grsic-Rausch, Thomas Rausch, Steffen Greiner*

Heidelberg Institute of Plant Sciences (HIP), Im Neuenheimer Feld 360, D-69120 Heidelberg, Germany

Received 23 September 2003; revised 10 November 2003; accepted 10 November 2003

First published online 25 November 2003

Edited by Ulf Ingo Flügge

Abstract Pectin methylesterases (PMEs) play an essential role during plant development by affecting the mechanical properties of the plant cell wall. Previous work indicated that plant PMEs may be subject to post-translational regulation. Here, we report the analysis of two proteinaceous inhibitors of PME in *Arabidopsis thaliana* (AtPMEI1 and 2). The functional analysis of recombinant AtPMEI1 and 2 proteins revealed that both proteins are able to inhibit PME activity from flowers and siliques. Quantitative RT-PCR analysis indicated that expression of AtPMEI1 and 2 mRNAs is tightly regulated during plant development with highest mRNA levels in flowers. Promotor::GUS fusions demonstrated that expression is mostly restricted to pollen.

Key words: Pectin methylesterase; Plant cell wall; Post-translational regulation; Functional genomics; *Arabidopsis thaliana*

1. Introduction

The plant cell wall is a highly complex structure, composed of polysaccharides, structural proteins and various enzymes. Besides cellulose and hemicellulose, pectins constitute a major portion of cell walls from dicot species accounting for ~35% of the primary cell wall dry weight [1]. Pectins are synthesized in the Golgi, methylesterified and modified with side chains and subsequently released into the apoplastic space as highly methylesterified polymers [2]. Those can later be modified, e.g., by pectin methylesterases (PMEs), which catalyze the demethylesterification of the homogalacturonan component of pectins [2]. This enzymatic activity of PMEs can lead either to cell wall loosening or to cell wall stiffening, depending on the apoplastic pH and the availability of divalent cations [2], thereby affecting shape and growth of plant cells. Manipulation of PME expression has been shown to influence physiological processes such as stem elongation and tuber yield [3], root development [4] and fruit softening [5].

Spatial and temporal regulation of PME activity during plant development is based on a large family of isoforms. In the *Arabidopsis* genome, 67 open reading frames (ORFs) are annotated as PMEs [2]. PME genes may be separated into two classes: type I genes contain two or three introns and the deduced proteins include a long pro-region, whereas type II genes contain five or six introns and the pro-region of the deduced proteins is missing in most cases [2]. Earlier studies revealed that expression of PME genes is strongly regulated in a tissue-specific manner [6–9].

Post-translational regulation of PMEs via proteinaceous inhibitors (PMEIs) represents another important control mechanism [10]. The first functionally and structurally characterized PMEI from kiwi fruit shows significant sequence homology to the well-characterized group of plant invertase inhibitors [11–13] and to the pro-region of type I PMEs [14]. Homology search revealed that in *Arabidopsis*, this newly discovered inhibitor protein family includes at least 14 genes, which may encode either PMEIs or invertase inhibitors [15]. However, some inhibitors might also have other target proteins. Both invertase inhibitors and PMEIs contain four cysteines at the same conserved positions which form two intramolecular disulfide bridges critical for protein folding [10,11]. Regarding these common structural features as well as the limited sequence conservation, comparisons based on the amino acid sequences alone do not allow to firmly assign a function to any of the proteins of this novel protein family. However, results from a phylogenetic analysis suggested that at1g47960 and at3g17130 might function as invertase inhibitors as they group with the functionally characterized tobacco invertase inhibitors [12,13], whereas at1g48020 and at3g17220 might represent PMEIs as deduced from their high sequence similarity with the kiwi fruit PMEI [15]. Here, we provide evidence that the genomic sequences at1g48020 and at3g17220 both indeed encode PMEI isoforms. In vitro proof of function for recombinant at1g48020 (AtPMEI1) and at3g17220 (AtPMEI2) proteins is presented. Furthermore, a detailed expression analysis indicates an important function during pollen development.

2. Materials and methods

2.1. Plant material

Arabidopsis thaliana cv Columbia plants were grown in the green house (9 cm pots) for 6 weeks under short-day conditions, and thereafter shifted to long-day conditions (2–3 weeks) for flower induction.

2.2. Cloning of AtPMEI1 and 2 expression plasmids

As at1g48020 (= AtPMEI1) and at3g17220 (= AtPMEI2) were predicted to be intron-free genes, the coding regions without the signal peptides (predicted by psort: http://psort.nibb.ac.jp/form.html with some adjustment according to the N-termini of known mature invertase inhibitors [16]) were amplified by polymerase chain reaction (PCR) from genomic DNA isolated from *A. thaliana* leaves according to [17], using the following primers: AtPMEI1, sense 5′-ATAGC-

*Corresponding author. Fax: (49)-6221-545859.
E-mail address: sgreiner@hip.uni-hd.de (S. Greiner).

0014-5793/03/$22.00
doi:10.1016/S0014-5793(03)01344-9

TAAATCCATGGACAGTTCAGAAATGAGCACAATC-3′, antisense 5′-AAATTGTCAAGGTACCTTAATTACGTGGTAACATG-TTAG-3′; AtPMEI2, sense 5′-ATAGCTAAATCCATGGTGGCA-GACATAAAAGCGAT-3′, antisense 5′-AAATTGTCAAGGTACC-TCACATCATGTTTGAGATGAC-3′. The amplification products were cloned into the pCR®4-TOPO® vector (TOPO TA Cloning Kit, Invitrogen), and subsequently excised with *Nco*I and *Kpn*I (RE sites underlined) and ligated into the *Nco*I/*Kpn*I restricted pETM-20 vector (http://www.embl-heidelberg.de/ExternalInfo/geerlof/draft_frames/flowchart/clo_vector/pETM/pETM-20.pdf), basically following the protocol established for the invertase inhibitor NtCIF [18]. Expression from this vector produces 6×His-tagged thioredoxin A-AtPMEI fusion proteins with a TEV protease cleavage site to separate the fusion partners after purification.

2.3. Expression and purification of recombinant AtPMEI1 and 2 proteins

The *Escherichia coli* strain Rosetta-gami™ (DE3) (Novagen, Madison, WI, USA) was used as host for protein expression. This strain is defective in thioredoxin reductase and glutathione reductase. Overnight cultures (37°C) were raised from single colonies. After 1:500 dilution with Luria–Bertani medium, bacteria were grown to a density of 0.6, induced by adding IPTG to 0.2 mM, and further grown for 24 h at 17°C. Thereafter, cells were pelleted for 15 min at 10 000×*g* and extracted with lysis buffer (1/20 volume of initial culture volume: 50 mM Na_2HPO_4/NaH_2PO_4, pH 7.0, 500 mM NaCl, 15 mM imidazole, 1% Triton X-100, 1 mg/ml lysozyme). After centrifugation at 45 000×*g* for 1 h, the supernatant was mixed with 2 ml of a 50% slurry of Ni-NTA resin (Qiagen, Hilden, Germany) and stirred at 4°C for 45 min before loading into a column. The column was first washed with 20 volumes of lysis buffer and then with 30 volumes of washing buffer (50 mM Na_2HPO_4/NaH_2PO_4, pH 7.0, 500 mM NaCl, 15 mM imidazole, 10% glycerol). Bound fusion protein was finally eluted with 10 volumes of the same buffer containing 250 mM imidazole, dialyzed against TEV protease cleavage buffer (50 mM Na_2HPO_4/NaH_2PO_4, pH 7.0, 200 mM NaCl), and thereafter cleaved with recombinant TEV protease for 3 h at 30°C. The untagged inhibitor proteins were separated from thioredoxin A and the protease with a second metal affinity chromatography step. Before use in invertase and PME inhibition assays, the recombinant proteins were dialyzed against buffer consisting of 20 mM triethanolamine and 7 mM sodium citrate, pH 4.8.

2.4. PME and acid invertase enzyme assays

An *Arabidopsis* PME preparation from a mixture of flowers and siliques was obtained by homogenizing the tissue in 2 ml/g extraction buffer [25 mM maleic acid/75 mM Tris-base, pH 7.0, 1 M NaCl, complemented with a complete mini EDTA-free protease inhibitor tablet (Roche, Mannheim Germany)]. After incubation on ice for 30 min with gentle agitation, the homogenate was centrifuged twice at 11 000×*g* for 10 min and the supernatant was kept to perform inhibition assays. PME activity was determined by a coupled enzymatic assay.

The assay was performed in 50 mM phosphate buffer, pH 7.5, in the presence of 0.4 mM NAD. PME activity with commercially available pectin (Sigma) as substrate is measured by determination of the produced methanol, which is first oxidized to formaldehyde by alcohol oxidase (1 U, Sigma), followed by oxidation to formiate via formaldehyde dehydrogenase (0.35 U, Sigma). The produced NADH was measured at $OD_{340\,nm}$ in a spectrophotometer.

Acid invertase activity (assay buffer: 30 mM sucrose, 20 mM triethanol amine, 7 mM citric acid, 1 mM phenyl methyl sulfonyl fluoride, pH 4.6) was measured by enzymatic determination of released glucose in a coupled assay with hexokinase and glucose-6-phosphate dehydrogenase [19].

For inhibition studies, enzyme preparations were mixed with recombinant AtPMEI proteins and coincubated in assay buffer without substrate for 30 min (PME assay) or 60 min (invertase assay). Thereafter, substrate was added and enzyme activity determined, assuring that time course and volume activities were in the linear range. As a control, PME or invertase preparations were preincubated without inhibitory proteins for the same period of time before activity measurement.

2.5. Transcript estimation by real-time PCR

Total RNA was extracted from various tissues of *A. thaliana* WT plants using the RNeasy Plant Mini Kit (Qiagen, Hilden, Germany), following the manufacturer's instructions. To eliminate residual genomic DNA present in the preparation, the samples were treated with RNase-free DNaseI (Promega, Mannheim, Germany) and the RNA was subsequently bound to RNeasy Spin columns (Qiagen) for purification. After elution with RNase-free water, 2 μg of RNA were transcribed into first strand cDNA using the Omniscript RT Kit from Qiagen with an oligo dT primer. Samples treated identically but without reverse transcriptase were used as a negative control in the PCR in order to exclude contamination with genomic DNA.

Real-time PCR was performed using the platinum Taq-DNA polymerase (Invitrogen, Karlsruhe, Germany) and SYBR-Green as fluorescent reporter in the Biorad iCycler. Primers were designed against the coding region of AtPMEI1 (sense 5′-CTACACAAGCGAGAGC-TAC-3′; antisense 5′-GTTCATCCCCATACCATCTCC-3′) and AtPMEI2 (sense 5′-CAAGACAGCAACCAACCCCACTATG-3′; antisense 5′-CAACCCTTTGCCATCGCCTGAC-3′). Primers against actin were described previously [20]. A serial dilution of flower cDNA was used as standard curve to optimize amplification efficiency for AtPMEI and actin primers. Each reaction was performed in triplicates, and specificity of amplification products was confirmed by melting curve and gel electrophoresis analysis. Relative expression levels of AtPMEI1 and AtPMEI2 were calculated and normalized with respect to Act2/8 mRNA according to the method in [21].

2.6. Generation of promoter::GUS plants

The promoter regions of AtPMEI1 and AtPMEI2 were amplified from genomic DNA with the following primers containing the GATEWAY cloning (Invitrogen, Karlsruhe, Germany) attB1 and attB2 sites: AtPMEI1, sense 5′-GGGGACAAGTTTGTACAAAAAAGC-AGCTAAGGGAACAAGGTATGTCACAC-3′, antisense 5′-GGG-GACCACTTTGTACAAGAAAGCTGGGTTCTTGTTTTCTCTAG-TAATTTTAG-3′; AtPMEI2, sense 5′-GGGGACAAGTTTGTA-CAAAAAAGCAGGCTTTCTTTAGATGTATCTTTCAC-3′, antisense 5′-GGGGACCACTTTGTACAAGAAAGCTGGGTCTTTG-CTTCTTTCTTTCTTAT-3′. GATEWAY cloning into the vector pBGWFS7 (http://www.psb.rug.ac.be/gateway/construct_list_plant.html) was performed following the manufacturer's instructions, and the correct insertion of the promoter region was confirmed by sequencing. The resulting vectors consisted of the promoter in front of an egfp/uidA gene fusion. After mobilizing the constructs in *Agrobacterium tumefaciens*, *A. thaliana* cv Columbia plants were transformed using the floral dip method [22]. Transformants were screened for resistance to the herbicide Basta™.

For analysis of GUS activity, tissue samples of T2 transformants were treated with GUS staining buffer (100 mM Na_2HPO_4/NaH_2PO_4, pH 7.0, 10 mM Na_2EDTA, 0.5 mM $K_3[Fe(CN)_6]$, 0.5 mM $K_4[Fe(CN)_6]$, and 0.08% X-GlucA (Duchefa, Haarlem, The Netherlands) for 16 h at 37°C. Green tissues were bleached with ethanol before examination.

3. Results and discussion

3.1. Heterologous expression of recombinant AtPMEI1 and 2 proteins and proof of function in vitro

To express AtPMEI1 and 2 as recombinant proteins, we followed a protocol established earlier for the invertase inhibitor NtCIF [18]. The predicted N-terminal signal sequences were deleted, and the remaining ORF cDNAs encoding the mature proteins were cloned into the pETM-20 vector. Expression from this vector in the *E. coli* strain Rosetta-gami™ yielded recombinant AtPMEI1 and 2 as N-terminal thioredoxin A-AtPMEI fusion proteins. AtPMEI1 and 2 were released by cleavage with TEV protease. As thioredoxin A and TEV protease are both provided with His-tags, the AtPMEI1 and 2 proteins enriched by negative purification were recovered in the flow-through of a Ni-affinity chromatography column (Fig. 1, lanes 1–3). The *E. coli* strain Rosetta-gami™ was chosen for its deficiencies in thioredoxin reductase and glutathione reductase activities, thus providing an oxidizing environment to facilitate disulfide bridge formation (see below).

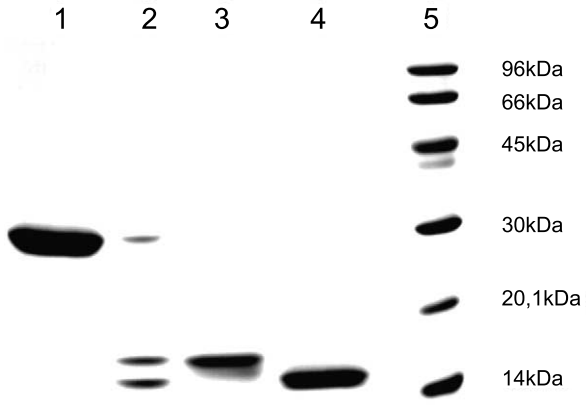

Fig. 1. Purification of soluble recombinant AtPMEI1 protein. Lane 1, purified fusion protein with thioredoxin A; lane 2, protein from lane 1 after TEV cleavage; lane 3, purified AtPMEI1 protein (flow-through after Ni-NTA chromatography); lane 4, same protein sample as in lane 3 but treated with non-reducing sample buffer; lane 5, molecular weight markers. Separation by SDS–PAGE on a 14% gel.

When purified, AtPMEI1 and 2 proteins were analyzed by sodium dodecyl sulfate–polyacrylamide gel electrophoresis (SDS–PAGE). Using sample buffer without reductant their mobility increased (Fig. 1, lanes 2 and 3), indicating the presence of intramolecular disulfide bridge(s) in the recombinant proteins. A similar shift was previously observed for the recombinant tobacco invertase inhibitor NtCIF [11]. Additionally, studies with NtCIF and kiwi PMEI proteins have shown that the correct folding of these inhibitor proteins is dependent on the formation of two intramolecular disulfide bridges [10,11]. Therefore, it was assumed that the AtPMEI1 and 2 proteins were correctly folded, and their in vitro activities were determined with four different target enzyme preparations, i.e. a PME preparation from *A. thaliana* flowers, a commercially available PME preparation from orange peel, a cell wall invertase (CWI) from tobacco suspension-cultured cells [19], and a vacuolar invertase (VI) isolated from *A. thaliana* leaves (Figs. 2 and 3).

The analysis of in vitro activities of recombinant AtPMEI1 and 2 clearly defined both proteins as inhibitors of PME. Conversely, both proteins showed no activities against CWI and VI preparations (Figs. 2 and 3). However, the bacterial PME from *Erwinia chrysanthemi* is not inhibited by recombinant AtPMEI1 and 2 proteins either (data not shown), making a role of PMEIs in pathogenesis unlikely. Interestingly, both inhibitors exhibited comparable activities against orange peel PME, whereas their activities clearly differed with *A. thaliana* flower PME as a target (Fig. 2). Here, AtPMEI1 was at least 10-fold more active as inhibitor. The essential role of the disulfide bridges in AtPMEI1 was demonstrated indirectly by comparing inhibitor activity of the recombinant protein with or without prior treatment with the reductant dithiothreitol (DTT). The preincubation with DTT completely

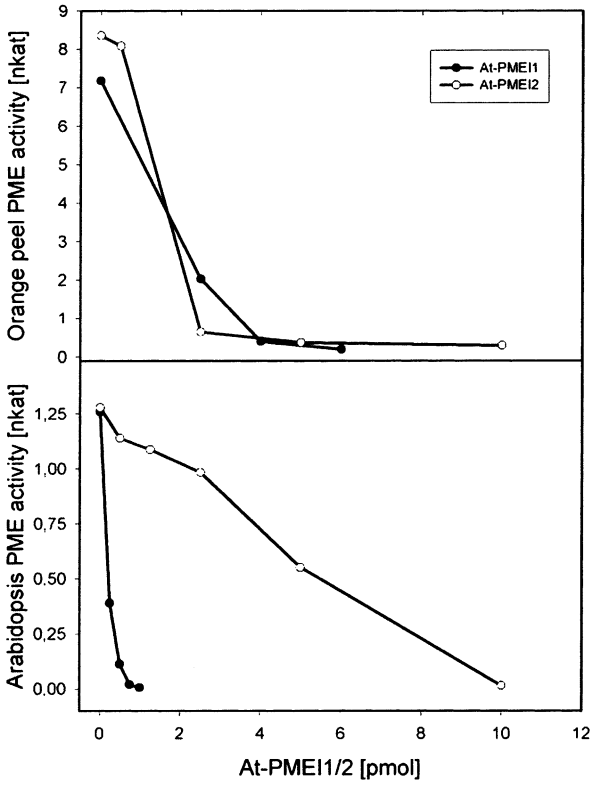

Fig. 2. Inhibitory effect of recombinant AtPMEI1 and 2 proteins on different PME preparations. The upper panel shows the dose-dependent inhibition of PME from orange peel (Sigma) by AtPMEI1 and AtPMEI2. The lower panel depicts the dose-dependent inhibition of an PME preparation from *Arabidopsis* (see Section 2). Target enzyme preparations were preincubated with inhibitor proteins for 30 min prior to enzyme assay.

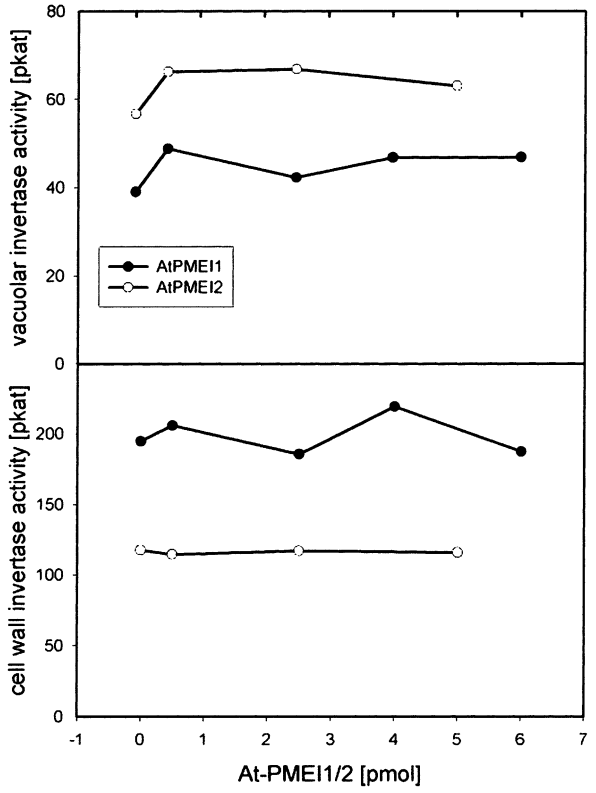

Fig. 3. No effect of recombinant AtPMEI1 and 2 proteins on VI and CWI. The upper panel depicts the dose-dependent effect of AtPMEI1 and AtPMEI2 on VI activity isolated from *Arabidopsis* leaves. The lower panel shows the effect of both AtPMEI proteins on a CWI preparation from tobacco suspension-cultured cells. Target enzyme preparations were preincubated with inhibitor proteins for 60 min prior to enzyme assay.

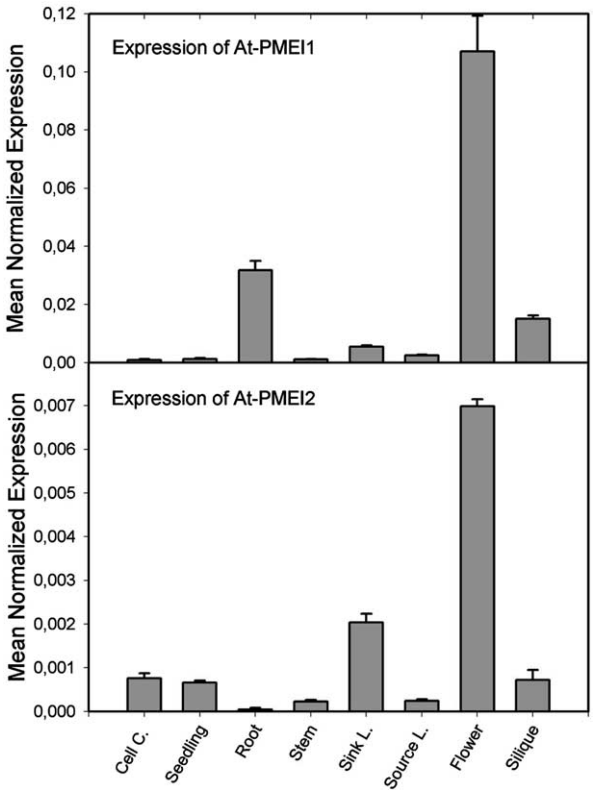

Fig. 4. Quantitative expression analysis of AtPMEI1 and 2 transcripts in different plant organs by real-time PCR. Upper panel, AtPMEI1; lower panel, AtPMEI2. Data are presented as relative expression normalized with respect to Actin2/8 mRNA (= 1). Tissue samples were collected from 8-week-old flowering plants (Cell C. = cell culture; Sink L. = sink leaf; Source L. = source leaf).
←

abolished inhibitor activity (data not shown). Analysis of AtPMEI1 activity in the range from pH 4.0 to pH 8.0, with *A. thaliana* flower PME as target, did not reveal a pronounced pH dependence (data not shown).

These results confirm earlier reports that individual members of the invertase inhibitor/PMEI protein family are either inhibitors of PME or invertases, but never both (S. Wolf, S. Grsic-Rausch, L. Camardella, S. Greiner and T. Rausch, unpublished results; [14]). The structural basis for this specificity remains unknown. We expect the structural model of the homologous NtCIF [23] to represent a scaffold that allows the investigation of these issues in three dimensions. A comparison of the protein sequences of AtPMEI1 and 2 with pro-regions of *A. thaliana* type I PMEs shows an overall sequence identity of up to 22% (AtPMEI1 with pro-region of at5g27870), with the four cysteines present in the conserved positions. It has been speculated that the pro-region could reflect an autoinhibitory domain [2]. As the pro-region is usually removed during PME maturation it remains unclear, whether AtPMEI1 and 2 interact with type I and/or type II PME enzymes. Heterologous expression of pro-regions is

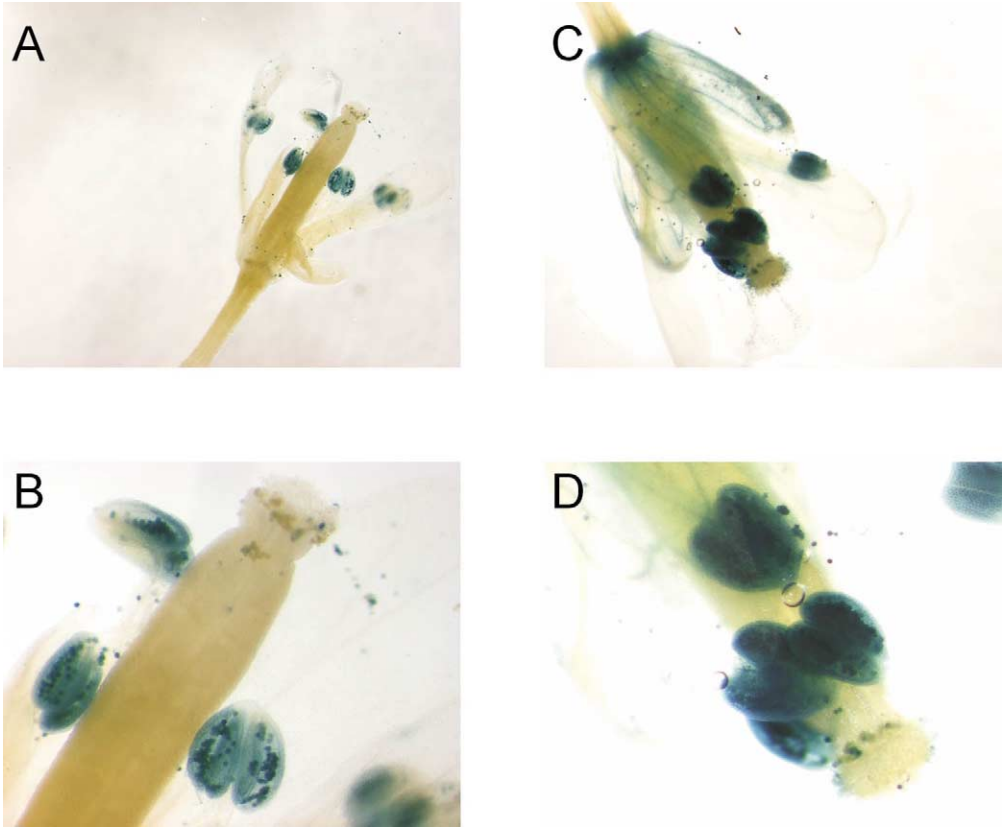

Fig. 5. Analysis of flower-specific expression of *AtPMEI1 and 2*, using promoter::GUS fusions. For *AtPMEI1*, pollen-specific expression is demonstrated in A and B. *AtPMEI2* also shows highest expression in pollen (C and D); however, GUS staining was also detected in the conducting tissues and the base of petals.

under way to characterize their interaction with mature PME enzymes in vitro.

3.2. Expression analysis by real-time PCR and promoter::GUS fusions

To compare the expression of AtPMEI1 and 2 mRNAs in different tissues, transcripts were quantitatively estimated by real-time PCR, using Actin2/8 for normalization (Fig. 4). The results revealed very low expression of both isoforms in most tissues except for flowers. The high expression in flowers was followed by root tissue for AtPMEI1 and by sink leaves for AtPMEI2. In general, AtPMEI2 showed a broader expression range than AtPMEI1. To explore the expression of AtPMEI1 and 2 in flowers at higher spatial resolution, we generated promoter::GUS lines for both isoforms, containing 667 and 524 bp of 5′-upstream sequence for AtPMEI1 and AtPMEI2, respectively (Fig. 5), with the 5′-ends of the promoter regions extending into the 3′-UTR of the neighboring annotated genes. The analysis of promoter::GUS transformants confirmed the results obtained by real-time PCR, showing no expression in most tissues for AtPMEI1, and low, but variable expression for AtPMEI2, whereas for both isoforms the high expression in flowers could be largely attributed to the anthers and pollen. Whereas AtPMEI1 expression appeared to be exclusively confined to anthers and pollen (Fig. 5A,B), GUS activity in AtPMEI2 promoter lines was also detected at the base and the conducting tissues of the sepals (Fig. 5C,D).

As far as we know, these data present the first systematic expression analysis of plant PMEI genes. As the PME protein family is highly complex (see Section 1), it is not yet possible to predict the target PME(s) of AtPMEI1 and 2. Our observations indicate that pollen-specific PME enzymes may be under post-translational control of inhibitor proteins. Note that in view of the high expression of AtPMEI1 and 2 in pollen, it is unclear whether the PME activity extracted from flowers and used as in vitro target enzyme in this study (see above) is the same PME isoform expressed in pollen. However, PME genes specifically expressed in pollen have been previously characterized for several plant species [8,9]. As during pollen formation and, in particular, during pollen tube growth the process of PME-mediated pectin deesterification appears to be under tight control, both spatially and temporally, an interaction of PME with PMEI proteins may be part of this regulation.

In more general terms, post-translational regulation of the apoplastically localized PME enzymes may, in view of the important spatial and temporal control of these enzymes for plant development, prove to be a mechanism similar to the post-translational control of CWI and VI enzymes by the structurally related inhibitor proteins. Studies of *A. thaliana* PMEI knock-out mutants are under way to further explore the role(s) of PMEI proteins during plant development.

Acknowledgements: The authors thank Emilia Sancho-Vargas for excellent technical assistance. Financial support of the KWS Saat AG and the Südzucker AG to T.R. and S.G. is gratefully acknowledged.

References

[1] Varner, J.E. and Lin, L.S. (1989) Cell 56, 231–239.
[2] Micheli, F. (2001) Trends Plant Sci. 6, 414–419.
[3] Pilling, J., Willmitzer, L. and Fisahn, J. (2000) Planta 210, 391–399.
[4] Wen, F., Zhu, Y. and Hawes, M. (1999) Plant Cell 11, 1129–1140.
[5] Brummell, D.A. and Harpster, M.H. (2001) Plant Mol. Biol. 47, 311–340.
[6] Micheli, F., Holliger, C., Goldberg, R. and Richard, L. (1998) Gene 220, 13–20.
[7] Harriman, R.W., Tieman, D.M. and Handa, A.K. (1991) Plant Physiol. 97, 80–87.
[8] Wakeley, P.R., Rogers, H.J., Rozycka, M., Greenland, A.J. and Hussey, P.J. (1998) Plant Mol. Biol. 37, 187–192.
[9] Li, Y.Q., Mareck, A., Faleri, C., Moscatelli, A., Liu, Q. and Cresti, M. (2002) Planta 214, 734–740.
[10] Camardella, L., Carratore, V., Ciardiello, M.A., Servillo, L., Balestrieri, C. and Giovane, A. (2000) Eur. J. Biochem. 267, 4561–4565.
[11] Greiner, S., Köster, U., Lauer, K., Rosenkranz, H., Vogel, R. and Rausch, T. (2000) Aust. J. Plant Physiol. 27, 807–814.
[12] Greiner, S., Krausgrill, S. and Rausch, T. (1998) Plant Physiol. 116, 733–742.
[13] Greiner, S., Rausch, T., Sonnewald, U. and Herbers, K. (1999) Nat. Biotechnol. 17, 708–711.
[14] Scognamiglio, M.A., Ciardiello, M.A., Tamburrini, M., Carratore, V., Rausch, T. and Camardella, L. (2003) J. Protein Chem. 22, 363–369.
[15] Rausch, T. and Greiner, S. (2004) Biochim. Biophys. Acta, in press.
[16] Weil, M., Krausgrill, S., Schuster, A. and Rausch, T. (1994) Planta 193, 438–445.
[17] Murray, M.G. and Thompson, W.F. (1980) Nucleic Acids Res. 8, 4321–4325.
[18] Hothorn, M., Bonneau, F., Stier, G., Greiner, S. and Scheffzek, K. (2003) Acta Crystallogr. D, in press.
[19] Weil, M. and Rausch, T. (1994) Planta 193, 430–437.
[20] Ha, S.B., Smith, A.P., Howden, R., Dietrich, W.M., Bugg, S., O'Connell, M.J., Goldsbrough, P.B. and Cobbett, C.S. (1999) Plant Cell 11, 1153–1163.
[21] Muller, P.Y., Janovjak, H., Miserez, A.R. and Dobbie, Z. (2002) BioTechniques 32, 1372–1379.
[22] Clough, S.J. and Bent, A.F. (1998) Plant J. 16, 735–743.
[23] Hothorn, M., D'Angelo, I., Marquez, J.A., Greiner, S. and Scheffzek, K. (2003) J. Mol. Biol., in press.